Experimental and Computational Study of the Gas-Phase Reaction of O(D-1) Atoms with VF5

ARTICLE *in* THE JOURNAL OF PHYSICAL CHEMISTRY A · JANUARY 2013

Impact Factor: 2.69 · DOI: 10.1021/jp3117616 · Source: PubMed

4 AUTHORS, INCLUDING:

Alexey Chichinin

Russian Academy of Sciences, Novosibirsk, Ru…

43 PUBLICATIONS **387** CITATIONS

SEE PROFILE

Vitaly G Kiselev

Russian Academy of Sciences

27 PUBLICATIONS **216** CITATIONS

SEE PROFILE

Nina Gritsan

Russian Academy of Sciences

168 PUBLICATIONS **2,061** CITATIONS

SEE PROFILE

THE JOURNAL OF PHYSICAL CHEMISTRY A

Article

pubs.acs.org/JPCA

Experimental and Computational Study of the Gas-Phase Reaction of O(^{1}D) Atoms with VF_5

Asylkhan A. Rakhymzhan,*[,†] Alexey I. Chichinin,[†,‡] Vitaly G. Kiselev,[†,‡] and Nina P. Gritsan[†,‡]

[†]Institute of Chemical Kinetics and Combustion SB RAS, 3 Institutskaya Str., Novosibirsk, 630090 Russia

[‡]Novosibirsk State University, 2 Pirogova Str., Novosibirsk, 630090 Russia

ABSTRACT: The reactions of O(^{1}D) atoms with VF_5 at room temperature have been studied by time-resolved laser magnetic resonance at the buffer gas (SF_6) pressure of 6 Torr. The O(^{1}D) atoms were produced by the photodissociation of ozone using an excimer laser (KrF, 248 nm). By monitoring the kinetics of FO radical formation, the bimolecular rate constant of O(^{1}D) consumption in collisions with VF_5 has been determined to be $k_{VF_5} = (7.5 \pm 2.2) \times 10^{-11}$ cm^3 s^{-1}. The branching ratio for the channel producing FO radicals (k_{8a}) has been found to be $k_{8a}/k_{VF_5} = 0.11 \pm 0.02$. Quantum chemical calculations at the CCSD(T)/CBS level of theory give evidence that the reactions of O(^{1}D) with VF_5 proceed via the VF_4OF intermediate. The enthalpy of the reaction leading to this intermediate formation was calculated to be −245.8 kJ/mol. In qualitative agreement with the experimental results, the reaction channel O(^{1}D) + VF_5 → FO + VF_4 (8a) turned out to be 72.9 kJ/mol energetically more favorable than the channel O(^{1}D) + VF_5 → F + OVF_4 (8b). The dissociation enthalpy of the OVF_4 radical was calculated to be very low (18.1 kJ/mol); hence, the decay of OVF_4 to F + OVF_3 should proceed very fast. The molecular channel O(^{1}D) + VF_5 → F_2 + VF_3O, though being most favorable thermodynamically, is kinetically unimportant.

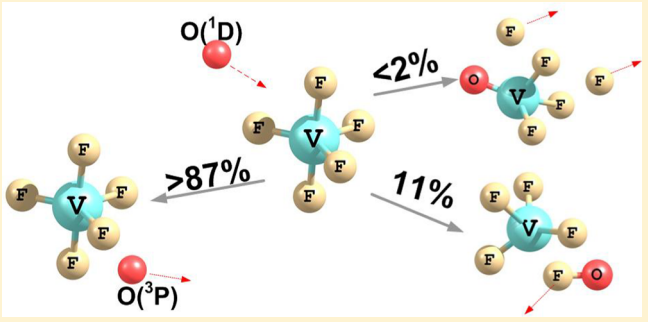

1. INTRODUCTION

Electronically excited oxygen atoms O(^{1}D) are important gas-phase atmospheric oxidants.[1,2] Particular attention has been paid to the reaction of O(^{1}D) atoms with polyatomic fluorides[1,3−5] as this reaction was recognized[3,4] to be a potentially key stratospheric loss process for the fluorinated saturated compounds − persistent greenhouse gases. In addition to the chemical reactions, O(^{1}D) atoms can be involved in the deactivation process via physical quenching. In the case of SO_2F_2, SF_5CF_3, SF_6, and C_nF_{2n+2} (n = 2−6), the collisional physical quenching was found to be the dominant channel of the O(^{1}D) loss.[1,5,6] At the same time, reactions of O(^{1}D) with F_2, XeF_2, and NF_3 proceed almost entirely by reactive quenching.[1,3,4] The latter is consistent with the exothermicity of the reactions leading to formation of FO radicals (Δ_rH^0 = −250.6,[3] −21.8,[3,7] and −45.6 kJ/mol[3] for F_2, XeF_2, and NF_3, respectively).

The present paper deals with reactivity of the singlet oxygen O(^{1}D) toward the vanadium pentafluoride, VF_5. The VF_5 is a highly volatile liquid (vapor pressure of 227 Torr at 300 K),[8] which has found application in industrial processes.[9−11] For instance, VF_5 is a key reagent in the synthesis of chladone-112, an industrial source of chladone-113, which, in turn, plays an important role in the manufacturing of fluoroplastics and fluororubbers.[12] Moreover, VF_5 is an extremely potent and promising oxidizer employed for selective oxidative fluorination of a variety of compounds (e.g., polyhalogenated arenes, alkenes, cycloalkenes, etc.) under mild conditions.[12−16] Apart from this, the VF_5 is a convinient photolytic source of fluorine atoms. It is indeed superior to widely used xenon difluoride (XeF_2), oxalyl fluoride $(FCO)_2$, and chlorine trifluoride (ClF_3). Among all of these species, the VF_5 has the largest absorption cross section at 248 nm (vide infra) and a very high vapor pressure. At the same time, the VF_4 radicals generated upon photolysis of VF_5 are stable species and are isolatable in the crystal state.[17,18] However, despite its application in the industrial processes and promising properties, the chemistry and photochemistry of VF_5 are still poorly understood.

In the present contribution, we report the kinetic results for the O(^{1}D) reaction with VF_5, which were obtained by monitoring the growth of the FO radical laser magnetic resonance (LMR) signal following the photolysis of VF_5 and ozone. The experimental findings have been rationalized with the aid of high-level quantum chemical calculations of several relevant stationary points on the potential energy surface for the O(^{1}D) + VF_5 system.

2. EXPERIMENTAL AND COMPUTATIONAL DETAILS

The LMR spectroscopy has been employed to monitor the kinetics of FO formation. Note that the IR absorption-based techniques, like LMR spectroscopy, are very convenient for the detection of FO radicals.[19] Detection of FO by microwave

Received: November 29, 2012
Revised: January 14, 2013
Published: January 14, 2013

spectroscopy is difficult due to a small dipole moment of this radical.[19,20] Application of the UV−vis spectroscopy is also inappropriate due to the predissociative nature of the FO electronic excited states.[19,20] The experimental setup and principles of the LMR spectroscopy are described in detail elsewhere.[21−24] Here, we will only briefly summarize the most relevant experimental details.

The FO radicals were detected using the 1033.49 cm^{-1} line of the $^{12}CO_2$ laser (vibration transition $\nu = 1 \leftarrow \nu = 0$ of the line 9P(34)) in the E⊥B polarization and the resonance magnetic field of 947 G.[23] The magnetic field was modulated at 120 kHz by a pair of coils mounted on the pole caps. The transient LMR signal was detected using a Ge−Hg photoresistor cooled by solid N_2 (53 K). The signal from a photoresistor was then detected by a lock-in amplifier at a frequency of the magnetic field modulation.

It should be emphasized that the amplitude of the LMR signal is proportional to the FO concentration only in the case of fast vibrational relaxation. To accelerate this process, the SF_6 buffer gas has been used. The choice of SF_6 was caused by the fact that it is inefficient in the deactivation of $O(^1D)$ atoms[5,25] but rather efficiently quenches the vibrational excitation of FO radicals

$$FO(\nu = 1) + SF_6(\nu_6 = 0) \xrightarrow{k_{1,0}} FO(\nu = 0) + SF_6(\nu_6 = 1) + 86\ cm^{-1} \quad (1)$$

where $k_{1,0} = (1.2 \pm 0.5) \times 10^{-11}$ cm^3 s^{-1}.[23] The fast relaxation of the FO radicals under experimental conditions was confirmed by the fact that the rise times of the "fast" FO LMR signals were close to the time resolution of the spectrometer (~4 μs) and by our estimations using the Schwartz−Slawsky−Herzfeld (SSH) model of vibrational relaxation as well.[26] According to this model, the time of relaxation from vibrational level ν_{max} to $\nu = 0$ can be estimated as $(1 + 1/2 + 1/3 + ... + 1/\nu_{max})/(k_{1,0}[SF_6])$. Under experimental conditions (P_{SF_6} = 6 Torr and ν_{max} = 10), this time is equal to 1.2 μs and is shorter than the time resolution of our LMR spectrometer. If one takes into account the anharmonicity, the relaxation will be even faster.

The $O(^1D)$ atoms were generated by laser-induced photodissociation of O_3.[27] The KrF excimer laser (248 nm, ~10 mJ/pulse) was used for excitation. All gases were manipulated in the copper and stainless steel vacuum lines equipped with Teflon rings. VF_5 and O_3 were injected into a flow of buffer gas (SF_6) a few centimeters before the gas mixture entered a Teflon cell. The typical concentrations of the substances used in our experiments were the following: $[O_3] = (3−30) \times 10^{14}$ cm^{-3}, $[VF_5] = (7−30) \times 10^{14}$ cm^{-3}, and $[SF_6] = 2 \times 10^{17}$ cm^{-3}. To avoid accumulation of the reaction products, all experiments were carried out under "slow flow" conditions. The linear flow rate through the reactor was about 50 cm/s, and the laser repetition rate was varied over the range of 1−5 Hz. Therefore, no part of the reaction mixture was subjected to more than a few laser shots.

The concentrations of O_3 and VF_5 were measured by mass flow meters and by UV photometry at 248 nm using the SF-26 spectrophotometer placed at the exit of the reaction cell. The concentration of ozone was also calculated from the rise time of the "slow" LMR signal, which is solely determined by the rate constant of the reaction of O_3 with fluorine atoms

$$F + O_3 \xrightarrow{k_2} FO^*(\nu \leq 10) + O_2 \quad (2)$$

The results of all of these measurements were in moderate agreement. For monitoring of the O_3 concentration, we used mainly the LMR signal rise time and the value of $k_2 = (1.0 \pm 0.3) \times 10^{-11}$ cm^3 s^{-1}.[28,29]

The tech-grade vanadium pentafluoride (the samples contained up to several percent of nonvolatile vanadium oxyfluoride (V) impurities) was kindly supplied by Prof. V. V. Bardin from the Novosibirsk Institute of Organic Chemistry. The UV absorption spectrum of VF_5 was recorded by a Shimadzu UV-2401PC spectrometer and was found to be in good agreement (Figure 1) with the literature.[30] Prior to use,

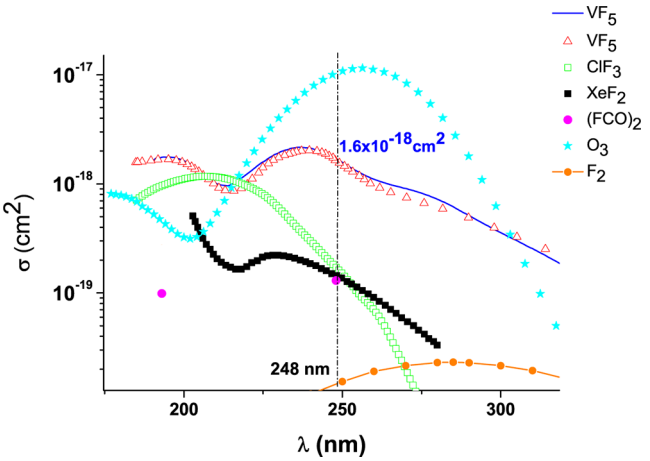

Figure 1. Experimental UV absorption spectrum of VF_5 (blue line, this work) and the reported UV absorption spectra of VF_5 (triangles, ref 30), ClF_3 (ref 53), XeF_2, (ref 54), and $(FCO)_2$, (ref 55).

the vanadium pentafluoride was placed in a stainless steel container and pumped at the liquid nitrogen temperature to purify from volatile impurities. Then, the mixture of 10% purified VF_5 and helium was employed in the experiments. The sample of VF_5 was recharged in the equilibrium vessel several times during the experiment. The ozone was produced from molecular oxygen in discharge at 77 K. After switching off the discharge, the remaining molecular oxygen was pumped away, and the mixture of ozone with helium (typically 15% O_3) was prepared. The highly pure SF_6 (better than 99.99%, Galogen, Russia) was used as a buffer gas.

Electronic structure calculations were carried out using the Gaussian 03[31] and Molpro 2009[32] program packages. The geometrical parameters of each structure were fully optimized using density functional theory at the B3LYP/6-311++G(2df,p) level.[33,34] All equilibrium and transition state structures were ascertained to be the minima and saddle points, accordingly, on the potential energy surfaces. The corresponding thermal corrections were included to obtain the enthalpy and Gibbs free energy values at room temperature. Single-point electronic energies were afterward refined using the coupled-cluster formalism CCSD(T)[35] in conjunction with the correlation-consistent aug-cc-pVnZ basis sets (n = T, Q).[36,37] For brevity, these basis sets are denoted henceforth as aVnZ. The Hartree−Fock and correlation components of the total CCSD(T) energies were separately extrapolated to the complete basis set (CBS) limit using the following two-point expressions:[38,39]

dx.doi.org/10.1021/jp3117616 | J. Phys. Chem. A 2013, 117, 814−820

$$E_{corr}(n) = E_{corr}^{CBS} + \frac{A}{n^3} \quad (3)$$

$$E_{HF}(n) = E_{HF}^{CBS} + B(n+1)\exp(-9\sqrt{n}) \quad (4)$$

where n = 3 and 4 for the aVTZ and aVQZ bases, respectively.[40]

3. RESULTS

3.1. UV Spectroscopy and Photochemistry of VF_5 and O_3. Figure 1 displays the UV spectrum of VF_5 along with the spectra of other selected photolytic precursors of the fluorine atom (F_2, XeF_2, ClF_3, and $(FCO)_2$). It is seen from Figure 1 that VF_5 has the largest absorption cross section (1.6×10^{-18} cm^2) among all of these precursors at the KrF laser excitation wavelength (248 nm).

According to the estimations on the basis of the literature thermodynamic data and our quantum chemical calculations

Table 1. Gas-Phase Enthalpies of Formation ($\Delta_f H^0_{gas}$ of the Selected Fluorosubstituted Vanadium Species

compound	$\Delta_f H^0_{gas}$, kJ/mol
VF_5	-1436.2 ± 0.8[a]
VF_3	-872 ± 10[b]
VF_3O	-1235 ± 30[c]
VF_4	-1261 ± 5[d]
VF_4O	-1156 ± 5[e]
FO	109 ± 10[f]
$F(^2P)$	79.4 ± 0.3[f]
$O(^3P)$	249.2 ± 0.1[f]
$O(^1D)$	438.1 ± 0.1[g]

[a]Reference 47. [b]A sum of $\Delta_f H^0_{solid}$ from ref 48 and the average of two values of $\Delta_{sub}H^0$ from refs 49 and 50. [c]Reference 51. Note that the authors pointed out that the value obtained might be subjected to serious errors. [d]Calculated using the experimental values for VF_5 and the fluorine atom and the CCSD(T)/CBS enthalpy $\Delta_r H^0_{gas}$ = 253.7 kJ/mol of the reaction $VF_5 \rightarrow VF_4 + F(^2P)$. Note that the experimental value $\Delta_f H^0_{gas} = -1200 \pm 25$ kJ/mol has been proposed in a very local and hard-to-access journal (ref 49). The reliability of this value is doubtful. [e]Calculated using the experimental $\Delta_f H^0_{gas}$ values for VF_5, oxygen, and fluorine atoms and the CCSD(T)/CBS enthalpy $\Delta_f H^0_{gas}$ of the reaction $VF_5 + O(^3P) \rightarrow OVF_4 + F(^2P)$ (cf. Figure 6). [f]Reference 52. [g]A sum of $\Delta_f H^0_{gas}$ of $O(^3P)$ from ref 52 and the experimental excitation energy (ref 44) $E(O(^3P) \rightarrow O(^1D))$.

(Table 1), two photochemical channels (radical and molecular) are exoergic upon the VF_5 excitation at 248 nm

$$VF_5 \xrightarrow{h\nu(248\ nm)} F + VF_4 \qquad \Delta E = 2.37\ eV \quad (5a)$$

$$F_2 + VF_3 \qquad \Delta E = 0.86\ eV \quad (5b)$$

where ΔE is the excess energy converting into the vibrational, rotational, and translation energies of the products in the ground electronic states. However, the quantum yield of fluorine atoms 5a is known to be close to unity (1.1 ± 0.4);[30] hence, the molecular channel 5b is most likely negligible.

Figure 1 shows that the ozone also efficiently absorbs the laser radiation. Excitation of O_3 at 248 nm yields mostly $O(^1D)$ atoms[6,41]

$$O_3 \xrightarrow{h\nu(248\ nm)} O(^1D) + O_2(^1\Delta) \quad (90\%) \quad (6a)$$

$$O(^3P) + O_2(^3\Sigma_g^-) \quad (10\%) \quad (6b)$$

The $O(^1D)$ is known to react with its precursor O_3

$$O(^1D) + O_3 \rightarrow 2O(^3P) + O_2(^1\Delta_g, {}^3\Sigma_g^-) \quad (7a)$$

$$\rightarrow 2O_2(^3\Sigma_g^-) \quad (7b)$$

with the overall rate constant $k_7 = (2.4 \pm 0.3) \times 10^{-10}$ cm^3 s^{-1}.[42]

A series of exothermic pathways can be proposed for the reaction of $O(^1D)$ atoms with VF_5

$$O(^1D) + VF_5 \longrightarrow FO + VF_4, \quad \Delta_r H^0_{gas} = -1.60\ eV, \quad (8a)$$

$$\longrightarrow F(^2P) + VF_4O, \quad \Delta_r H^0_{gas} = -0.81\ eV, \quad (8b)$$

$$\downarrow$$

$$2F(^2P) + VF_3O, \quad (8c)$$

$$\longrightarrow F_2 + VF_3O, \quad \Delta_r H^0_{gas} = -2.46\ eV, \quad (8d)$$

$$\longrightarrow O(^3P) + VF_5, \quad \Delta_r H^0_{gas} = -1.96\ eV, \quad (8e)$$

the enthalpies of these processes were estimated using the values given in Table 1. The fluorine atoms produced both upon excitation of VF_5 (pathway 5a) and by its reaction with $O(^1D)$ (pathways 8b and 8c) react with ozone, yielding FO radicals (reaction 2).

Other reactive species, $O_2(^1\Delta_g)$, $O_2(^3\Sigma_g^-)$, and $O(^3P)$, are formed in reactions 6 and 7. However, the reactions of these species with VF_5 are endoergic, and we did not include them in the reaction scheme. Apart from this, the only overall exoergic reaction can be proposed (Table 1)

$$VF_4 + O_3 \rightarrow VF_3O + O_2 + F \qquad \Delta_r H^0_{gas} = -0.37\ eV \quad (9)$$

Nevertheless, we believe that the contribution of this process to the production of the F atoms to be negligible in comparison with the pathways 8b and 8c due to its relatively low exothermicity and chemical stability of the VF_4 radical. Furthermore, all secondary radical−radical reactions were neglected as they are unimportant on a time scale of our experiment (few milliseconds).

3.2. Kinetics of the FO Radical Formation. The concentrations of $O(^1D)$ and F atoms produced upon photolysis of O_3 and VF_5 at 248 nm can be calculated using formulas 10 and 11, respectively

$$[O(^1D)]_0 = \Omega\Phi_{O^*/O_3}\sigma(O_3)[O_3] \quad (10)$$

$$[F]_0 = \Omega\Phi_{F/VF_5}\sigma(VF_5)[VF_5] \quad (11)$$

where $\sigma(O_3) = 1.08 \times 10^{-17}$ cm^2 (ref 41) and $\sigma(VF_5) = 1.6 \times 10^{-18}$ cm^2 are the corresponding absorption cross sections (Figure 1), $\Phi_{O^*/O_3} = 0.9$[41] and $\Phi_{F/VF_5} = 1.1 \pm 0.4$[30] are the quantum yields of $O(^1D)$ and F atoms, and Ω is a number of the UV photons per laser pulse divided into the area of the laser beam. As a matter of fact, only the ratio $\gamma = (\Phi_{F/VF_5} \times \sigma(VF_5))/(\Phi_{O^*/O_3} \times \sigma(O_3)) = 0.16$ has been used in the quantitative analysis of the experimental data.

dx.doi.org/10.1021/jp3117616 | J. Phys. Chem. A 2013, 117, 814−820

As follows from the kinetic scheme (reaction 8), the concentrations of FO radicals and F atoms just after the completion of $O(^1D)$ decay ($[FO]_1$ and $[F]_1$) are given by the expressions

$$[FO]_1 = k_{8a}/k_f[O(^1D)]_0[VF_5] \quad (12)$$

$$[F]_1 = k_{8bc}/k_f[O(^1D)]_0[VF_5] \quad (13)$$

$$k_f = k_{O_3}[O_3] + k_{VF_5}[VF_5] \quad (14)$$

where $k_{8b} < k_{8bc} \lesssim 2k_{8b}$ (see section 3.4), $k_{O3} \equiv k_7$, k_f denotes the pseudo-first-order rate constant for the overall process of the $O(^1D)$ deactivation by O_3 and VF_5, and $k_{VF_5} = k_{8a} + k_{8bc} + k_{8d} + k_{8e}$. We did not take into account the deactivation of $O(^1D)$ by SF_6 as it has a very low rate constant ($<2 \times 10^{-14}$ cm^3 s^{-1}).[5] Even at the lowest concentrations of O_3 and VF_5 used in this study, the contribution of the deactivation by SF_6 was estimated to be less than 10%.

The concentration of FO radicals produced in the reaction of F atoms with O_3 (reaction 2) is labeled by index 2 and is given by the expression 15. We assume here that each F atom produces one FO radical due to reaction 2.

$$[FO]_2 = [F]_0 + [F]_1 \quad (15)$$

This reaction is 10−100 times slower than the deactivation of $O(^1D)$ atoms; hence, the $[FO]_1$ and $[FO]_2$ concentrations can be easily identified from the biexponential kinetics of FO growth. Typically, the LMR signal of FO radicals rises rapidly during the first several microseconds and reaches the amplitude S_1, which corresponds to the concentration $[FO]_1$. The signal continues to grow slowly and reaches a plateau at 50−600 μs after the laser pulse; then, it decays over several milliseconds. The amplitude of the slow part of the signal growth is denoted S_2, and the concentration at the plateau corresponds to the $[FO]_1 + [FO]_2$ value.

It is reasonable to assume that $S_1 = \alpha[FO]_1$ and $S_2 = \alpha[FO]_2$, where α is a constant that corresponds to the sensitivity of our spectrometer to the FO radicals. Using eqs 10−15, the following expression can be derived for the ratio of the amplitudes S_2 and S_1:

$$\frac{S_2}{S_1} = \gamma\frac{k_{VF_5}[VF_5]}{k_{8a}[O_3]} + \gamma\frac{k_{O_3}}{k_{8a}} + \frac{k_{8bc}}{k_{8a}} \quad (16)$$

The S_2/S_1 ratio has been measured in the two sets of experiments. In the first case, the concentration of ozone was fixed, and $[VF_5]$ was varied in the range of $(6–20) \times 10^{14}$ cm^{-3}. In the second series of experiments, the concentration of VF_5 was fixed, and $[O_3]$ was varied in the range of $(2–30) \times 10^{14}$ cm^{-3}. According to eq 16, the plots of S_2/S_1 versus either $[VF_5]$ or $[O_3]^{-1}$ should be linear with a slope proportional to k_{VF_5}/k_{8a}. In turn, the value of $(\gamma k_{O_3}/k_{8a} + k_{8bc}/k_{8a})$ can be extracted from the intercept of linear plots.

As follows from eqs 10, 12, and 14, the experimental dependences of the fast signal amplitude (S_1) on the ozone concentration can be fitted by an expression with parameters c and d

$$S_1 = \frac{c[O_3]}{d + [O_3]} \quad (17)$$

The fitting parameter $d = (k_{VF_5}/k_{O_3})$ $[VF_5]$ can be used to obtain k_{VF_5}, the sum of the rate constants of all channels 8a−8e of the $O(^1D)$ atom deactivation by VF_5.

3.3. Analysis of the Experimental Kinetics. Figure 2 displays the typical kinetic curve of the LMR signal growth. The kinetics consists of the fast initial step followed by slow exponential growth reaching a plateau. On a longer time scale (several milliseconds), the decay of the LMR signal is observed. This decay is most likely due to the recombination of FO radicals.

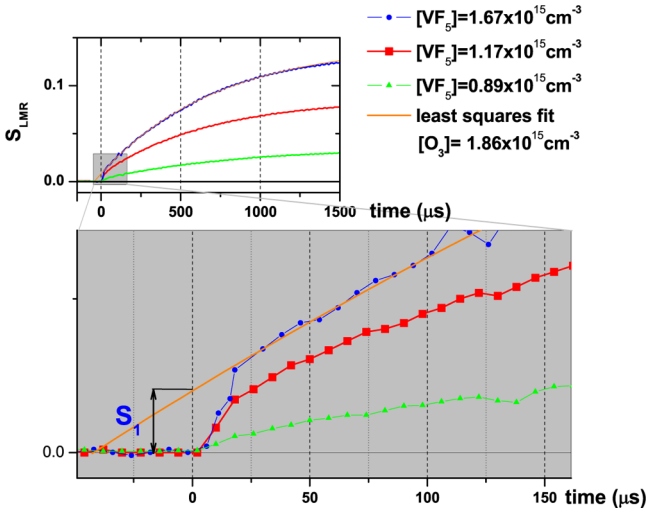

Figure 2. The typical time dependence of the LMR signal recorded after 248 nm excitation of O_3/VF_5 mixtures at 6 Torr of SF_6.

Unfortunately, the time resolution of our setup is insufficient for the measurement of a rise time of the fast initial step. Actually, this rise time is determined by the lock-in amplifier. In turn, the slow component of the kinetics is well-described by the exponential function. This time dependence was extrapolated to the zero time, and the amplitude of the slow component and its intercept (Figure 2) were taken as the values of S_2 and S_1, respectively. Recall that the time constants of the slow component have been used for the evaluation of the ozone concentration.

Figure 3 presents the dependence of the ratio S_2/S_1 on the reciprocal ozone concentration ($[O_3]^{-1}$). These data have been measured in a series of experiments with the constant VF_5 concentration ($[VF_5] = 6 \times 10^{14}$ cm^{-3}). In turn, Figure 4 displays the dependence of the same ratio S_2/S_1 on the concentration of VF_5 obtained in a series of experiments with a constant concentration of ozone ($[O_3] = 1.1 \times 10^{14}$ cm^{-3}). Figures 3 and 4 demonstrate that the linear dependence (eq 16) indeed fits well the experimental data. The values of the ratio k_{8a}/k_{VF_5} determined from the slopes of Figures 3 and 4 were found to be in good agreement with each other and were equal to 0.11 ± 0.02.

Figure 5 presents a typical plot of the S_1 value versus ozone concentration. The least-squares fitting of this plot by expression 17 yields the values of the parameters c and d. Consequently, using the values of d and k_3, we were able to determine $k_{VF_5} = (7.5 \pm 2.2) \times 10^{-11}$ cm^3 s^{-1}.

Figures 3 and 4 show a relatively large value (5.0 ± 0.2) of the intercept. This intercept is described by a sum of the second and third terms of eq 16. Using the values of k_{VF_5} and k_{8a}

dx.doi.org/10.1021/jp3117616 | J. Phys. Chem. A 2013, 117, 814−820

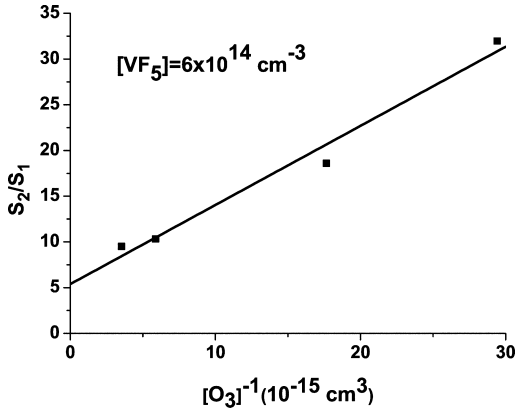

Figure 3. The typical plot of the S_2/S_1 ratio versus reciprocal of the ozone concentration ($[O_3]^{-1}$) at a constant value of the VF_5 concentration ($[VF_5] = 6 \times 10^{14}$ cm^{-3}, points) and the linear fitting of the data according to eq 16.

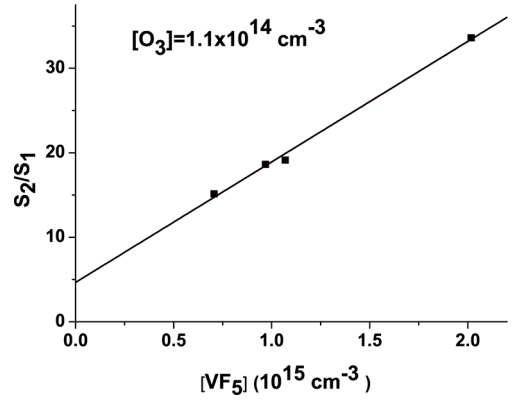

Figure 4. The typical plot of the S_2/S_1 ratio versus VF_5 concentration at a constant value of $[O_3] = 1.1 \times 10^{14}$ cm^{-3} (points) and the linear fitting of the data according to eq 16.

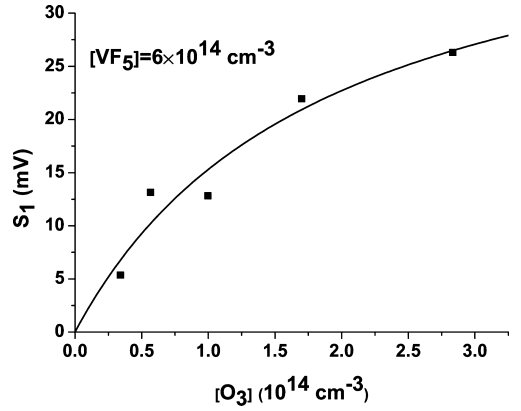

Figure 5. The typical dependence of the "fast signal amplitude" (S_1) on the ozone concentration $[O_3]$ and the best fitting of the data by eq 17.

obtained above, the second term can roughly be estimated as ~4.7. However, the accuracy of both this value (±50%) and the intercept (±0.2) is too poor to evaluate the third term of eq 16 in a reliable way ($k_{8bc}/k_{8a} = 0.3^{+2.3}_{-0.3}$). Nevetheless, we believe the branching ratio to be $k_{8bc}/k_{8a} \ll 1$. In order to rationalize this assumption, we used quantum chemical calculations (vide infra).

We also tried to detect the reaction $O(^1D) + SF_6 \rightarrow FO + SF_5$ upon photolysis of the O_3/SF_6 mixtures (the concentration of SF_6 was varied up to 6×10^{17} cm^{-3}). Unfortunately, we were unable to detect the LMR signal of FO in these experiments. Therefore, the upper limit of the rate constant of this reaction was estimated to be 10^{-14} cm^3 s^{-1}. The low value of this rate constant is reasonable taking into account the endothermicity of the reaction ($\Delta_r H^0$ = 100.4 kJ/mol).[43]

3.4. Quantum Chemical Calculations. In order to get deeper insight into the branching ratios of the channels 8a–8d, we performed quantum chemical calculations of some relevant stationary points on the singlet PES of the VF_5O system (Figure 6). Because the excited state $O(^1D)$ has a strong

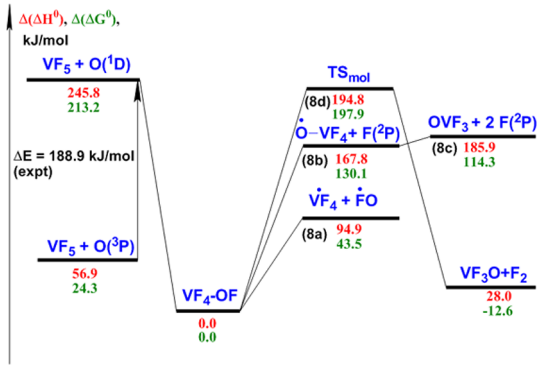

Figure 6. The relative thermodynamic parameters of some stationary points on the PES corresponding to the reactions of the $VF_5 + O(^1D)$ system. The VF_4OF intermediate was chosen as a reference compound for the calculations of the relative thermodynamic properties. All values are in kJ/mol and are calculated at the CCSD(T)/CBS level of theory.

multireference character, we computed at the CCSD(T)/CBS level of theory the electronic energy corresponding to the ground state $O(^3P)$. This value was combined with the well-established experimental excitation energy $E(O(^3P) \rightarrow O(^1D))$ (188.9 kJ/mol).[44] As seen from Figure 6, the very thermodynamically favorable VF_4OF intermediate, which lies 245.8 kJ/mol below the $VF_5 + O(^1D)$ asymptote, is readily formed upon collision of VF_5 with $O(^1D)$. In contrast to the oxide F_3VO, which is a stable compound, we were unable to find a minimum corresponding to the oxide F_5VO. In the latter case, all optimizations resulted in a structure of VF_4OF.

Prior to thermalization, the F_4VOF intermediate with a large excess of energy (~245 kJ/mol, Figure 6) will undergo fast decay according to the pathways 8a–8e. The results of Figure 6 show that the molecular decomposition reaction 8d leading to VF_3O and F_2 is thermodynamically the most favorable channel. However, the activation enthalpy of this reaction is about 200 kJ/mol (Figure 6). Therefore, the molecular channel 8d is not feasible kinetically. In contrast to the molecular channel, the radical channels are barrierless. The computations undoubtedly indicate that the most thermodynamically preferable radical channel of VF_4OF decomposition leads to the formation of VF_4 and FO radicals (channel 8a). The products of the competing radical channel 8b, namely, OVF_4 and the F atom, lie 72.9 kJ/mol higher on the enthalpy scale (Figure 6).

According to the RRKM theory,[45] the branching ratio k_{8b}/k_{8a} can be estimated as the ratio of the numbers of rovibronic levels in the transition states (TSs) for these channels. Obviously, the number of states in the TS for the channel 8a having an excess

dx.doi.org/10.1021/jp3117616 | J. Phys. Chem. A 2013, 117, 814–820

energy of ~150 kJ/mol is profoundly larger than that for channel 8b with ~80 kJ/mol of excess energy. Thus, the ratio k_{8b}/k_{8a} is much less than unity.

At the same time, the product of reaction 8b, namely, VF_4O, is prone to dissociation, yielding an additional F atom. The enthalpy of this process was calculated to be $\Delta_r H^0 = 18.1$ kJ/mol (Figure 6). We were unable to localize the TS for this reaction and hypothesize that the dissociation is a barrireless process. Taking into account the very low endothermicity of this reaction, we suppose that the dissociation of VF_4O occurs much faster than its formation from the intermediate VF_4OF with the large excess of energy (Figure 6). Thus, the two F atoms are produced with the rate constant k_{8b}, and consequently, $k_{8bc} \simeq 2k_{8b}$. In this case, the branching ratio is $k_{8bc}/k_{8a} \ll 1$ (cf. the previous section).

Therefore, we infer that channel 8a is responsible for the reactive quenching of $O(^1D)$. At the same time, the contribution of this channel to the overall deactivation of $O(^1D)$ by VF_5 is about 11%. Thus, the deactivation of $O(^1D)$ by VF_5 is mainly determined by physical quenching with the rate constant $k_{8e} = (6.7 \pm 1.9) \times 10^{-11}$ cm^3 s^{-1}, which is about 1/3 of the collision rate constant.

3.5. Comparison of $O(^1D)$ Reactions with VF_5 and NF_3. The most studied reaction of $O(^1D)$ deactivation is its chemical quenching by NF_3.[2,3,6,46] The rate constant of this reaction, $(2.0 \pm 0.3) \times 10^{-11}$ cm^3 s^{-1}, is noticeably lower than k_{VF_5} measured in this paper. In contrast to our case, the deactivation of $O(^1D)$ by NF_3 proceeds almost entirely by reactive quenching (>83%,[3] ~99%[6]). Two radical channels leading to formation of F atoms (eq 18a) and FO radicals (eqs 18b and 18c) have been proposed for these reactions.[2,3,6,46]

$$O(^1D) + NF_3 \rightarrow ONF_3 \rightarrow F + ONF_2 \quad (18a)$$

$$\rightarrow FONF_2 \rightarrow FO + NF_2 \quad (18b)$$

$$\rightarrow F_2NF\cdots O \rightarrow FO + NF_2 \quad (18c)$$

In our previous study[3], we detected directly the formation of FO radicals and concluded that the channel (eqs 18b,18c) is the dominant. However, recently, Dillon et al.[2] reinvestigated this reaction, detecting luminescence of OH radicals generated in the reaction of F atoms with water. In contrast to our findings, the authors proposed the F and ONF_2 to be the primary products (channel 18a). At present, it remains an unexplained discrepancy, but we are in progress of measuring accurately the ratio $k_{18a}/(k_{18b} + k_{18c})$.

Reaction 18a proceeds through the intermediacy of trifluoroamine oxide, ONF_3, which is formed in the barrierless addition of $O(^1D)$ to NF_3.[2,3,6,46] The ONF_3 is a well-known stable species, and its formation is a highly exoergic process ($\Delta_r H^0 = -433$ kJ/mol).[2,46] This intermediate has a very large excess of internal energy and decomposes very quickly prior to vibrational relaxation.

Computational studies[2,46] suggest two types of intermediates for channels 18b and 18c. The FO radical might be formed in the dissociation of the F_2NOF intermediate (channel 18b), which, in turn, is formed through the isomerization of ONF_3.[3,46] However, the insertion of $O(^1D)$ into the N−F bond has been later rejected due to a high activation barrier,[2] the isomerization of ONF_3 to F_2NOF has been questioned, and the formation of a weak prereactive $F_2NF\cdots O$ complex has been proposed (channel 18c). Note that all stationary points (and TSs) on the PES were localized using DFT at the M05-2X level.[2] In our opinion, the high-level multireference calculations (e.g., CASSCF/CASPT2) have to be performed to elucidate the mechanism of the primary reactions of $O(^1D)$. On the other hand, the methods employed indeed yield accurate thermodynamics of the processes (channels 18a−18c). It was found that the formation of the F atom is more favorable than the FO radical ($\Delta H_{0K} = 90.0$ kJ/mol).[2]

Nevertheless, the reaction of $O(^1D)$ with VF_5 qualitatively differs from that with NF_3. Recall that in the case of VF_5, the physical quenching is a major process of $O(^1D)$ deactivation, and its rate constant is close to 1/3 of the collision rate constant. Unfortunately, more sophisticated calculations are required to analyze physical quenching (e.g., the estimations of the spin−orbit coupling (SOC) at the conical intersection of the singlet and triplet PES). However, it is reasonable to expect stronger SOC in the case of the VF_5O system containing a heavier vanadium atom.

Moreover, in contrast to NF_3, there are no minima on the PES corresponding to the pentafluorovanadium oxide, F_5VO. The reason for this is a steric hindrance caused by the five fluorine substituents. Indeed, the vanadium oxytrifluoride F_3VO is a stable compound similar to the oxide F_3NO. Thus, in the case of VF_5, both radical reactions proceed through the F_4VOF intermediate, and contrary to the $O(^1D) + NF_3$ case, the formation of the FO radical is thermodynamically much more preferable than that of the F atom (Figure 6).

4. CONCLUSION

In this study, the formation of FO radicals upon the 248 nm laser flash photolysis (LFP) of the mixture of VF_5 and O_3 has been directly detected by time-resolved LMR spectroscopy. The two pathways leading to FO radicals were identified, the reaction of the $O(^1D)$ with VF_5 (the "fast" process) and the reaction of fluorine atoms with O_3 (the "slow" process). In turn, the fluorine atoms are formed by both the LFP of VF_5 and its reaction with $O(^1D)$.

The sum of the rate constants of all reactions between VF_5 and $O(^1D)$ (the rate constant of deactivation) has been measured to be $k_{VF_5} = (7.5 \pm 2.2) \times 10^{-11}$ cm^3 s^{-1}, and the branching ratio for the radical reactive channels yielding FO radicals has been determined to be 0.11 ± 0.02.

A deep minimum corresponding to the VF_4OF intermediate has been localized on the PES for the reaction of $O(^1D)$ with VF_5. The enthalpy of the reaction leading to this intermediate was calculated to be −245.8 kJ/mol at the CCSD(T)/CBS//B3LYP/6-311++G(2df,p) level of theory. We were unable to localize other intermediates (e.g., OVF_5) or transient complexes on this PES. The minor radical channel $O(^1D) + VF_5 \rightarrow F + OVF_4$ (channel 8b) was found to be 72.9 kJ/mol thermodynamically less favorable than the main radical channel $O(^1D) + VF_5 \rightarrow FO + VF_4$ (channel 8a). The dissociation enthalpy of VF_4O was found to be negligibly small ($\Delta_r H^0 = 18.1$ kJ/mol). Most likely, the decay $VF_4OF \rightarrow F + VF_4O$ is followed by the dissociation of VF_4O to $F + VF_3O$. The molecular reactive channel $O(^1D) + VF_5 \rightarrow F_2 + OVF_3$ was found to be the most favorable thermodynamically. However, this reaction proceeds through a very high activation barrier and cannot compete with the radical channels.

dx.doi.org/10.1021/jp3117616 | J. Phys. Chem. A 2013, 117, 814−820

AUTHOR INFORMATION

Corresponding Author

*E-mail: rakhymzhan@kinetics.nsc.ru.

Notes

The authors declare no competing financial interest.

ACKNOWLEDGMENTS

The authors greatly acknowledge Prof. V. V. Bardin for the supply of vanadium pentafluoride and helpful discussions. This work was supported by the Russian Foundation for Basic Research (Projects 12-03-31741 and 12-03-31363). The support of this work by the Siberian Supercomputer Center is gratefully acknowledged.

REFERENCES

(1) Baasandorj, M.; Hall, B. D.; Burkholder, J. B. *Atmos. Chem. Phys. Discuss.* **2012**, *12*, 24011−24042.
(2) Dillon, T.; Vereecken, L.; Horowitz, A.; Khamaganov, V.; Crowley, J. N.; Lelieveld, J. *Phys. Chem. Chem. Phys.* **2011**, *13*, 18600−18608.
(3) Sorokin, V.; Gritsan, N. P.; Chichinin, A. I. *J. Chem. Phys.* **1998**, *108*, 8995−9003.
(4) Clyne, M.; Watson, R. *Chem. Phys. Lett.* **1971**, *12*, 344−346.
(5) Ravishankara, A.; Solomon, S.; Turnipseed, A.; Warren, R. *Science* **1993**, *259*, 194−199.
(6) Zhao, Z.; Laine, P. L.; Nicovich, J. M.; Wine, P. H. *Proc. Natl. Acad. Sci. U.S.A.* **2010**, *107*, 6610−6615.
(7) Johnson, G. K.; Malm, J.; Habbard, W. N. *J. Chem. Thermodyn.* **1972**, *4*, 879−891.
(8) Clark, H. C.; Emeleus, H. J. *J. Chem. Soc.* **1957**, 2119−2122.
(9) Redshaw, C. *Dalton Trans.* **2010**, *39*, 5595−5604.
(10) Gibson, V.; Spitzmesser, S. *Chem. Rev.* **2003**, *103*, 283−315.
(11) Hagen, H.; Boersma, J.; van Koten, G. *Chem. Soc. Rev.* **2002**, *31*, 357−364.
(12) Krasilnikov, V. A.; Andreev, G. G.; Karelin, A. I.; Guzeeva, T. I.; Furin, G. G.; Bardin, V. V.; Avramenko, A. A. *Zh. Prikl. Khim.* **1994**, *67*, 1891−1893.
(13) Furin, G. G.; Bardin, V. V. In *New Fluorinating Agents for Organic Synthesis*; German, L. S., Zemskov, S. V., Eds.; Springer: New York, 1989; Chapter 4, pp 117−139.
(14) Yagupolskii, L. M. In *Houben-Weyl Methods of Organic Chemistry. Organo-Fluorine Compounds*, 4th ed.; Baasner, B., Hagemann, H.; Tatlow, J.-C., Eds.; Thieme: Stuttgart, Germany, 2000; Vol. *E10a*; Chapter 12, pp 509−534.
(15) Bardin, V. V.; Bardina, S. G. *J. Fluorine Chem.* **2004**, *125*, 1411−1414.
(16) Krespan, C. G.; Petrov, V. A. *Chem. Rev.* **1996**, *96*, 3269−3302.
(17) Cavell, R. G.; Clark, H. C. *J. Chem. Soc.* **1962**, 2692−2698.
(18) Becker, S.; Miiller, B. G. *Angew. Chem., Int. Ed. Engl.* **1990**, *29*, 406−407.
(19) McKellar, A. R. W. *Canad. J. Phys.* **1979**, *57*, 2106−2113.
(20) Langhoff, S.; Bauschlicher, C., Jr.; Partridge, H. *Chem. Phys. Lett.* **1983**, *102*, 292−298.
(21) Rakhymzhan, A.; Chichinin, A. *J. Phys. Chem. A* **2010**, *114*, 6586−6593.
(22) Chichinin, A.; Chasovnikov, S.; Krasnoperov, L. *Chem. Phys. Lett.* **1987**, *138*, 371−376.
(23) Chichinin, A.; Krasnoperov, L. *Chem. Phys.* **1990**, *143*, 281−296.
(24) Chichinin, A. I. *J. Chem. Phys.* **2000**, *112*, 3772−3779.
(25) Davidson, J.; Sadowski, C.; Schiff, H.; Streit, G.; Howard, C.; Jennings, D.; Schmektekopf, A. *J. Chem. Phys.* **1976**, *64*, 57−62.
(26) Schwartz, R.; Slawsky, Z.; Herzfeld, K. *J. Chem. Phys.* **1952**, *20*, 1591−1960.
(27) Chowdhury, A. M. S. *Laser Phys.* **1999**, *9*, 959−989.
(28) Bedzhanyan, Y. R.; Markin, E. M.; Gershenzon, Y. M. *Kinet. Catal.* **1993**, *33*, 594−601.
(29) Nielsen, O. J.; Sehested, J. *Chem. Phys. Lett.* **1993**, *213*, 433−441.
(30) Petrov, N.; Chebotaev, N.; Pshezhetsky, S. *Quantum Electron.* **1977**, *4*, 2248−2251.
(31) Frisch, M. J.; Trucks, G. W.; Schlegel, H. B.; Scuseria, G. E.; Robb, M. A.; Cheeseman, J. R.; Scalmani, G.; Barone, V.; Mennucci, B.; Petersson, G. A.; et al. *Gaussian 03*, revision C.02; Gaussian Inc.: Wallingford, CT, 2004.
(32) Werner, H.-J.; Knowles, P. J.; Knizia, G.; Manby, F. R.; Schutz, M.; Celani, P.; Korona, T.; Lindh, R.; Mitrushenkov, A.; Rauhut, G.; et al. *MOLPRO*, version 2010.1, a package of ab initio programs; 2010.
(33) Becke, A. *J. Chem. Phys.* **1993**, *98*, 5648−5652.
(34) Lee, T.; Yang, W.; Parr, R. *Phys. Rev. B* **1988**, *37*, 785−789.
(35) Pople, J. A.; Head-Gordon, M.; Raghavachari, K. *J. Chem. Phys.* **1987**, *87*, 5968−5965.
(36) Dunning, T. H. *J. Chem. Phys.* **1989**, *90*, 1007−1023.
(37) Balabanov, N. B.; Peterson, K. A. *J. Chem. Phys.* **2005**, *123*, 064107.
(38) Kutzelnigg, W.; Morgan, J. D. *J. Chem. Phys.* **1992**, *96*, 4484−4508.
(39) Karton, A.; Martin, J. M. L. *Theor. Chem. Acc.* **2006**, *115*, 330−333.
(40) Note that we also extrapolated the CCSD(T) energies using the three-point expression $E(n) = A_{CBS} + B_{exp}(-(n-1)) + C_{exp}(-(n-1)^2)$, where n = 2, 3, and 4 for the aVnZ bases, D, T, and Q, respectively. The difference between the two approaches did not exceed 2 kJ/mol.
(41) Sander, S. P.; Friedl, R. R.; Golden, M., D.M. and Kurylo; Moortgat, G.; Keller-Rudek, H.; Wine, P. H.; Ravishankara, A.; Kolb, C.; Molina, M.; Finlayson-Pitts, B.; Huie, R.; Orkin, V. *JPL Publication 06-2*; NASA: Pasadena, CA, 2006.
(42) Dunlea, E.; Ravishankara, A. *Phys. Chem. Chem. Phys.* **2004**, *6*, 2152−2161.
(43) Tsang, W.; Herron, J. T. *J. Chem. Phys.* **1992**, *96*, 4272−4282.
(44) Moore, C. E. In *Tables of Spectra of Hydrogen, Carbon, Nitrogen, and Oxygen*; Gallagher, J. W., Ed.; CRC Press, Inc.: Boca Raton, FL, 1993.
(45) Holbrook, A.; Pilling, M.; Robertson, S. In *Unimolecular Reactions*, 2nd ed.; Robinson, P. J., Ed.; John Wiley & Sons Ltd, Chichester, U.K., 1996; p 417.
(46) Antoniotti, P.; Grandinetti, F. *Chem. Phys. Lett.* **2002**, *366*, 676−682.
(47) Johnson, G.; Hubbard, W. *J. Chem. Thermodyn.* **1974**, *6*, 59−63.
(48) Marley, N. F.; Johnson, G. K. *II. Vanadium Trifluoride*; Chem. Eng. Div. Thermochem. Studies No. ANL-76-102, Argonne Natl. Lab.: Argonne, Illinois, 1976; pp 14−17.
(49) Igolkina, N.; Nikitin, M.; Boltalina, O.; Sidorov, L. *High Temp. Sci.* **1986**, *21*, 111−117.
(50) Sidorov, L. N.; Denisov, M. Y.; A., A. P.; Shtolz, V. B. *Zh. Fiz. Khim.* **1966**, *40*, 1151−1154.
(51) Flesch, G. D.; Svec, H. J. *Inorg. Chem.* **1975**, *14*, 1817−1822.
(52) Chase, M. W. *NIST-JANAF Thermochemical Tables, Monograph 9, Part I, II*, 4th ed.; National Institue of Standards and Technology: Gaithersburg, MD, 1998.
(53) Sorokin, V. I.; Chichinin, A. I. *Chem. Phys. Lett.* **1997**, *280*, 141−144.
(54) Black, G.; Sharpless, R. L.; Lorents, D. C.; Huestis, D. L.; Gutcheck, R. A.; Bonifield, T. D.; Helms, D.; Walters, G. K. *J. Chem. Phys.* **1981**, *75*, 4840−4846.
(55) Badenes, M.; Castellano, E.; Cobos, C.; Croce, A.; Tucceri, M. *Chem. Phys.* **2000**, *253*, 205−217.